Arterial calcifications and increased expression of vitamin D receptor targets in mice lacking TIF1α

Mihaela Ignat, Marius Teletin, Johan Tisserand, Konstantin Khetchoumian, Christine Dennefeld, Pierre Chambon*, Régine Losson*, and Manuel Mark*

Institut de Génétique et de Biologie Moléculaire et Cellulaire, Centre National de la Recherche Scientifique, Institut National de la Santé et de la Recherche Médicale, Université Louis Pasteur, BP 10142, 67404 Illkirch Cedex, France

Contributed by Pierre Chambon, December 21, 2007 (sent for review December 12, 2007)

Calcification of arteries is a major risk factor for cardiovascular mortality in humans. Using genetic approaches, we demonstrate here that the transcriptional intermediary factor 1α (TIF1α), recently shown to function as a tumor suppressor in murine hepatocytes, also participates in a molecular cascade that prevents calcifications in arterioles and medium-sized arteries. We further provide genetic evidence that this function of TIF1α is not exerted in hepatocytes. The sites of ectopic calcifications in mutant mice lacking TIF1α resemble those seen in mice carrying an activating mutation of the calcium sensor receptor (*Casr*) gene and, in *TIF1α*-deficient kidneys, *Casr* expression is increased together with that of many other vitamin D receptor (VDR) direct target genes, namely *Car2*, *Cyp24a1*, *Trpv5*, *Trpv6*, *Calb1*, *S100g*, *Pthlh*, and *Spp1*. Thus, our data indicate that TIF1α represses the VDR pathway in kidney and suggest that an up-regulation of *Casr* expression in this organ could account for ectopic calcifications generated upon *TIF1α* deficiency. Interestingly, the calcifying arteriopathy of *TIF1α*-null mutant mice shares features with the human age-related Mönckeberg's disease and, overall, the *TIF1α*-null mutant pathological phenotype supports the hypothesis that aging is promoted by increased activity of the vitamin D signaling pathway.

aging | ectopic calcification | mouse knockout | transcriptional regulation | vitamin D signaling

Initially identified through its ability to interact directly with nuclear receptors in a ligand-dependent manner, transcriptional intermediary factor 1 (TIF1α), also known as tripartite motif (TRIM24) protein, was subsequently described as both a negative and positive regulator of ligand-induced transactivation acting through chromatin modification (1–6).

To address the physiological functions of TIF1α, we monitored large cohorts of *TIF1α*-deficient (*TIF1α*$^{-/-}$) mice. Hepatic tumors were detected at necropsy in a vast majority of *TIF1α*$^{-/-}$ mutants, thus indicating that *TIF1α* deficiency predisposes to liver tumor formation. Tumor predisposition was not observed in *TIF1α*$^{-/-}$ mutants heterozygous for the retinoic acid receptor α (*Rara*) gene, thereby providing genetic proof that *TIF1α* and *Rara* act in opposition to each other in liver carcinogenesis (6).

In the present study, a systematic histological analysis of *TIF1α*$^{-/-}$ mutants at different ages was carried out to examine the effect of *TIF1α* gene deletion on a wide range of tissues. This analysis revealed that, aside from occasional metastases from liver tumors (6), *TIF1α*$^{-/-}$ mutants displayed calcifications, increasing with age, in extra-hepatic connective tissues, namely arterioles, medium-sized arteries, lungs, and vibrissae. These ectopic calcifications were correlated with an increase in expression of several vitamin D direct targets, therefore raising the possibility that TIF1α could repress the vitamin D receptor (VDR) signaling pathway *in vivo*.

Results

Calcifications of Renal Arteries and Arterioles in Young *TIF1α*$^{-/-}$ Mutants. Tissues of 2-month-old *TIF1α*$^{-/-}$ mutants were indistinguishable from those of age-matched WT littermates (data not shown). In contrast, hematoxylin/eosin staining of kidney sections at 3 months of age revealed deposits of an acellular, basophilic (i.e., taking up hematoxylin), material (C; compare Fig. 1 *B* with *A*) in about three-fourths of the *TIF1α*$^{-/-}$ males and females, but never in age-matched WT littermates. These abnormal deposits were restricted to glomerular arterioles and medium-sized (i.e., hilar and arcuate) arteries and spared the veins that often bordered an affected artery. They contained calcium, stained in brown by the von Kossa method, (C; compare Fig. 1 *D* and *F* with *C* and *E*), but did not take up the lipid-soluble dye oil red O and thus did not represent atherosclerotic plaques. No extrarenal ectopic calcification was detected in 3-month-old *TIF1α*$^{-/-}$ mutants.

Extensive Calcifications of Arterioles, Arteries, Vibrissae, and Lungs in Old *TIF1α*$^{-/-}$ Mutants. Histological sections of 8- to 10-month-old *TIF1α*$^{-/-}$ mutants showed calcifications in arterioles and medium-sized (i.e., muscular) arteries with an incidence of 100% in kidney (Fig. 1 *I* and *J*) and tongue (Fig. 1*G*), 6% in brown fat (Fig. 1*H*), 13% in snout dermis, 20% in heart, 30% in retina, and 65% in thyroid. It is noteworthy that these percentages underscore the actual extent of arterial calcifications as they were established through analysis of a single section of each organ. The fact that calcifications were detected in only 30% of histological sections through limb muscles, but were consistently observed in alizarin red-stained whole-mount preparations (C in Fig. 1 *M–O*), supports this statement. We did not detect arterial calcifications in muscular arteries supplying liver, spleen, lung, and testis. Importantly, no calcification was ever detected in large (i.e., elastic) arteries including aorta and its major branches (data not shown), whereas calcified foci were scarce in major arteries supplying limbs (i.e., humeral and femoral arteries; e.g., Ah; Fig. 1*N*), in sharp contrast with their branches of smaller caliber (A in Fig. 1 *M–O*). Altogether, these observations indicate that the extent of the pathological mineralization process is negatively correlated to the caliber of arteries and, consequently, that it spares the large vessels forming the bed of atherosclerotic plaques.

Calcifications in lungs and vibrissae affected 100% and 88% of the 8- to 10-month-old *TIF1α*$^{-/-}$ mutants, respectively. In lungs, calcifications were confined to alveolar walls and displayed features characteristic of pulmonary alveolar microlithiasis (C in Fig. 2*B* and refs. 7 and 8). In vibrissae, mineralization was restricted to the capsules (CA in Fig. 2 *D*, *F*, and *H*). Age-matched WT littermates did not show evidence of ectopic calcified deposit at any sites (Figs. 1*L* and 2 *A*, *C*, *E*, and *G*),

Author contributions: M.I., M.T., R.L., and M.M. contributed equally to this work; R.L., and M.M. designed research; M.I., M.T., J.T., K.K., and C.D. performed research; M.I., M.T., J.T., K.K., P.C., R.L., and M.M. analyzed data; and P.C., R.L. and M.M. wrote the paper.

The authors declare no conflict of interest.

*To whom correspondence may be addressed. E-mail: chambon@igbmc.u-strasbg.fr, losson@igbmc.u-strasbg.fr, or manuel.mark@igbmc.fr.

This article contains supporting information online at www.pnas.org/cgi/content/full/0712030105/DC1.

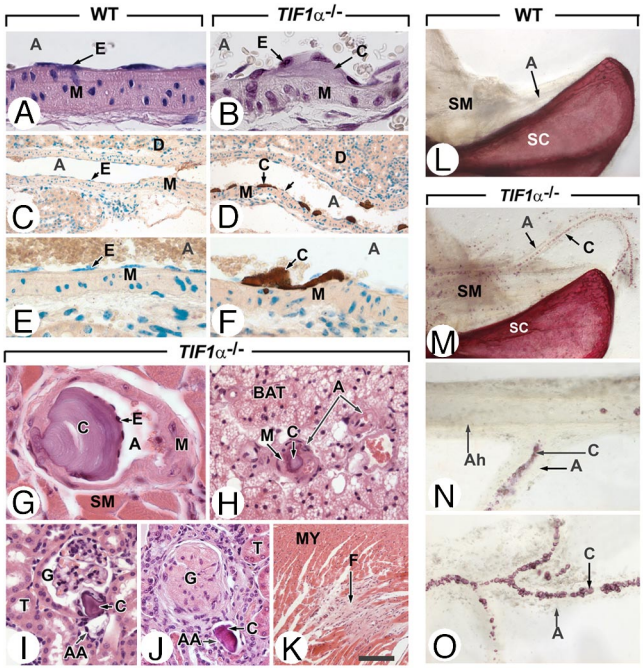

Fig. 1. Ectopic calcifications in medium-sized arteries and arterioles of *TIF1α*$^{-/-}$ mutants. (*A–F*) Longitudinal histological sections through branches of renal arteries of 3-month-old WT and *TIF1α*$^{-/-}$ mutants, stained with hematoxylin/eosin (*A* and *B*) or the von Kossa method for detection of calcified deposits (brown color) and DAPI (green nuclear stain) (*C–F*). (*G–K*) Sections through different organs in 10-month-old *TIF1α*$^{-/-}$ mutants stained with hematoxylin/eosin. (*G*) Tongue: this photomicrograph illustrates the hallmarks of calcified deposits in medium-sized arteries namely, acellularity, localization between endothelium and smooth muscles of the media, propensity to develop within arterial lumens, apparent intactness of their covering endothelial cell layer and absence of accompanying inflammatory cell infiltrates. (*H*) Interscapular brown fat showing an arteriole that is completely blocked by a calcified ''plug.'' (*I* and *J*) Calcified deposits in the arterioles of kidney glomeruli result in glomerulosclerosis (in *J*). (*K*) Myocardial fibrosis most probably corresponding to a scar from an ancient ischemic focus. (*L–O*) Whole-mount preparations of bones and muscles of 10-month-old WT and *TIF1α*$^{-/-}$ mutants stained with the calcium dye alizarin red. In *N* and *O* note the striking inverse correlation between the density of calcified deposits and the caliber of forelimb arteries. Note that the photomicrographs of whole-mount preparations in *L* and *M* and in *N* and *O* were taken at identical magnifications. A, artery or arterial lumen; Ah, humeral artery; AA, afferent arterioles of kidney glomeruli; BAT, brown adipose tissue; C, calcified deposits; E, endothelium; G, kidney glomerulus; F, fibrotic myocardium; M, arterial smooth muscles; MY, cardiomyocytes; SM, striated (i.e., voluntary) muscles; T, kidney tubules. (Scale bar: *A*, *B*, and *G*,16 μm; *C* and *D*, 80 μm; *E*, *F*, *H*, *I*, and *J*, 40 μm; *K*, 160 μm.)

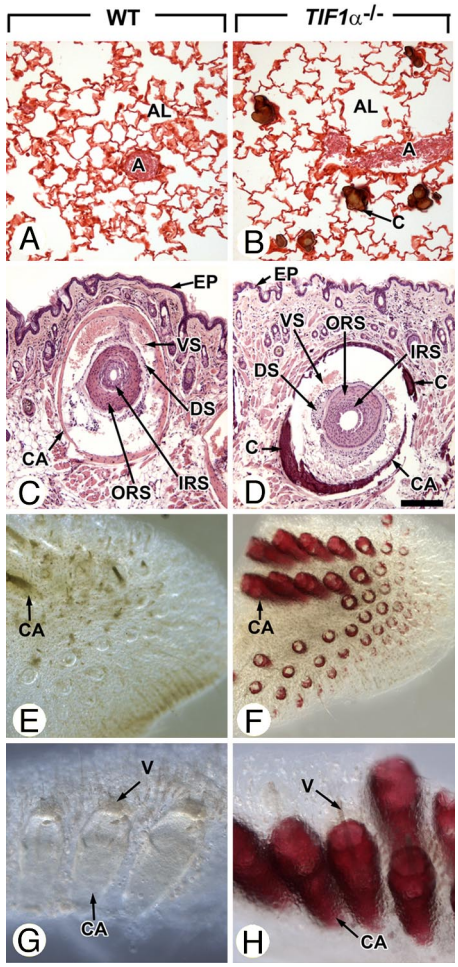

Fig. 2. Ectopic calcifications of lungs and vibrissae in 10-month-old *TIF1α*$^{-/-}$ mutants. (*A–D*) Histological sections through lungs and vibrissae of *TIF1α*$^{-/-}$ mutants and age-matched WT littermates stained by using the von Kossa method (brown calcified deposits) and either safranin 0 (*A* and *B*) or hematoxylin/eosin (*C* and *D*). (*A* and *B*) Note that calcified nodules are restricted to the *TIF1α*$^{-/-}$ mutant alveoli, are not associated with inflammatory cell infiltrates, and spare the lung arterial bed. (*C* and *D*) Transverse sections through vibrissae surrounded by blood vessel sinuses (VS), which are themselves encased by a muscular capsule (CA). (*E–H*) Low (*E* and *F*) and high (*G* and *H*) high-magnification views of whole-mounts of muzzle skin stained with alizarin red confirm extensive mineralization of vibrissae capsules in *TIF1α*$^{-/-}$ mutants. Note that photomicrographs of whole-mounts in *E* and *F* and in *G* and *H* were taken at identical magnifications. A, arteries; AL, lung alveoli; C, calcified deposits; CA, capsules of vibrissae; DS, ORS and IRS, dermal sheath, outer root sheath and inner root sheath of the vibrissae, respectively; EP, epidermis; V, vibrissae; VS, blood vessel sinuses of the vibrissae. (Scale bar: *A* and *B*, 80 μm; *C* and *D*, 160 μm.) (Magnifications: *E* and *F*, ×10; *G* and *H*, ×60.)

thereby excluding the possibility that the genetic background of the mouse line could predispose to soft tissue mineralization. As to tissues that are normally calcifying, it should be stressed that skeletons of 3-month-old *TIF1α*$^{-/-}$ males were undistinguishable from their WT counterparts in terms of size and shape of bones and tracheal rings, and that histopathological analysis of *TIF1α*$^{-/-}$ tibia growth plates revealed a normal organization of their layers (data not shown).

Our histological analysis of the tissues listed in *Materials and Methods* revealed noncalcified lesions only in kidneys and myocardium. In about one-third of 8- to 10-month-old *TIF1α*$^{-/-}$ mutants, kidneys displayed scattered foci of glomerulosclerosis (compare G in Fig. 1 *I* and *J*), and sections through their myocardium occasionally showed areas of fibrosis (F in Fig. 1*K*). These lesions, which were never observed in WT littermates, were most probably caused by arteriolar occlusions (e.g., Fig. 1*J*). Quite surprisingly, owing to the extent of vascular calcifications, there was no sign of ischemic injury to voluntary muscles (data not shown).

Normal Blood Parameters in *TIF1α*$^{-/-}$ Mutants. *TIF1α*$^{-/-}$ mutants at 8 months of age had calcium and phosphate serum concentrations within the normal range (Table 1). These data rule out hypercalcemia and hyperphosphatemia as causes of ectopic calcifications and therefore suggest that the *TIF1α*$^{-/-}$ mutants pathology is not a disease of parathyroid origin. Mutant blood cell counts were normal [supporting information (SI) Table 3].

In humans, chronic renal failure, manifested by an elevation in serum creatinine levels, is associated with ectopic calcifications attributable, in part, to hyperphosphatemia (reviewed in refs. 9 and 10). In this context, the fact that *TIF1α*$^{-/-}$ mutants

Table 1. Serum biochemical profiles in WT (*TIF1α*$^{+/+}$) and *TIF1α*$^{-/-}$ mice (means ± SD) at the age of 8 months

	Female mice		Male mice	
Factor	WT	TIF1α	WT	TIF1α
Glucose, mmol/liter	4.79 ± 1.09	3.87 ± 0.73	6.53 ± 1.30	6.23 ± 1.85
Phosphorus, mmol/liter	2.64 ± 0.64	2.18 ± 0.19	2.72 ± 0.16	2.62 ± 0.22
Calcium, mmol/liter	2.43 ± 0.17	2.40 ± 0.15	2.45 ± 0.06	2.51 ± 0.18
Urea, mmol/liter	9.84 ± 2.34	8.27 ± 1.54	10.30 ± 2.39	10.10 ± 1.19
Creatinine, μmol/liter	43.50 ± 3.78	39.67 ± 3.27	43.25 ± 7.59	44.33 ± 4.84
Cholesterol, mmol/liter	2.61 ± 0.65	2.14 ± 0.37	3.13 ± 0.50	3.45 ± 0.35
Triglyceride, mmol/liter	1.52 ± 0.37	1.65 ± 0.64	2.16 ± 0.88	2.31 ± 0.25
Protein, g/liter	57.33 ± 3.79	56.75 ± 6.45	58.50 ± 2.12	65.00 ± 4.24
Free fatty acids, mEq/liter	1.54 ± 0.39	1.43 ± 0.1	1.01 ± 0.18	1.92 ± 0.13
ASAT, units/liter	192.67 ± 90.43	148.83 ± 49.81	164.50 ± 67.27	182.83 ± 131.69
ALAT, units/liter	51.00 ± 20.07	62.67 ± 31.62	83.50 ± 64.42	76.33 ± 37.33
LDH, units/liter	1,051.17 ± 448.16	896.00 ± 368.75	1,054.50 ± 632.40	1,183.83 ± 544.27

n = 5 mice of each genotype and gender. ASAT, aspartate aminotransferase; ALAT, alanine aminotransferases; LDH, lactate dehydrogenase.

suffering from glomerulosclerosis had normal circulating creatinine levels (Table 1) proved that their rate of glomerular filtration was not significantly decreased.

The Function of TIF1α in Preventing Arterial Calcifications Is Not Exerted in Hepatocytes. Hepatocytes, which represent major targets of the *TIF1α*-null mutation (6), are known to secrete inhibitors of calcium deposition in soft tissues (11–13). Thus, we investigated whether inactivating *TIF1α* solely in hepatocytes would induce calcification of kidney arteries. To this end, mice harboring floxed alleles of *TIF1α* (defined as *TIF1α*$^{L2/L2}$ mice) were crossed with *Alb-Cre* transgenic mice that express Cre exclusively in hepatocytes to generate *TIF1α*$^{L2/L2}$ *Alb-Cre* mice, in which TIFα is ablated in all hepatocytes at 6 weeks of age (*TIF1α*$^{hep-/-}$ mice; ref. 6 and references therein). All 10 *TIF1α*$^{hep-/-}$ mice analyzed at 3 months of age displayed the liver abnormalities characteristic of the *TIF1α*$^{-/-}$ mutation in the germ line (i.e., in the whole organism) (6). In contrast, none of these *TIF1α*$^{hep-/-}$ mutant mice displayed calcifications of kidney vessels (data not shown). This observation rules out the possibility that the ectopic calcification phenotype of *TIF1α*$^{-/-}$ mutants is a systemic disease of liver origin.

TIF1α Deficiency Increases the Expression of Vitamin D Target Genes Involved in Calcium Homeostasis in the Kidney. As the kidney arterial bed is the earliest target organ of *TIF1α* deficiency-induced calcifications, we next focused our investigations on expression, in kidney, of genes involved in calcium homeostasis. To this end, total kidney RNA of 3-month-old *TIF1α*$^{-/-}$ mutant and WT littermates was analyzed by quantitative RT-PCR. In *TIF1α*$^{-/-}$ mutants, mRNA levels of *Casr* (encoding a calcium-sensing receptor), *Cyp24a1* [encoding the 25-hydroxyvitamin D-24-hydroxylase that controls intracellular levels of 1,25$(OH)_2$D3], *Trpv5* and *Trpv6* (encoding calcium-regulating ion channels), *Calb1* and *S100g* (encoding calcium-binding proteins), *Spp1* (encoding the secreted phosphoprotein 1, osteopontin), *Abcc6* (encoding a transmembrane transporter of the multidrug resistance protein family), *Pthlh* (encoding the parathyroid hormone-like peptide), and *Car2* (encoding carbonic anhydrase type 2) all were significantly up-regulated (Fig. 3*A*). On the other hand, genes expressed in WT kidneys and not implicated in calcium homeostasis, namely *Aldh1a3*, *Wt1*, *and Epo*, were not significantly altered in their expression levels in kidneys lacking TIF1α ($P > 0.05$; Fig. 3*A*). Altogether, these results indicate that the *TIF1α*-null mutation selectively increases, in kidney, the expression levels of numerous genes involved in calcium homeostasis. Among these, *Car2*, *Cyp24a1*, *Casr*, *Trpv5*, *Trpv6*, *Calb1*, *S100g*, *Spp1*, and *Pthlh* are known to be direct vitamin D targets (refs. 14–18 and references therein). Therefore, their increased expression in *TIF1α*-deficient kidneys indicates that TIF1α down-regulates the vitamin D pathway in kidney.

TIF1α Is Expressed in Tissues Exerting Crucial Functions in Calcium Homeostasis, but Is Undetectable in Endothelial Cells. In *TIF1α*$^{-/-}$ mutants, ectopic calcifications developed in contact with endothelial cells lining the lumen of arteries and arterioles, making up the bulk of the lung alveolar wall or forming the interface between capsules and blood sinuses of vibrissae. Endothelial cells therefore represented good candidates as primary targets of the *TIF1α* null mutation. However, TIF1α could not be detected in endothelial cells or in vascular smooth muscle cells by immunohistochemistry on sections of WT mice, whereas it was present in a variety of epithelial cells types (Fig. 3, Table 2, and SI Fig. 4). These data indicate that TIFα may act in tissues known to play critical roles in calcium homeostasis and expressing the VDR, namely renal tubules and glomeruli (T and G in Fig. 3 *B* and *C*), intestinal epithelium, and parathyroid gland parenchyma (Table 2, SI Fig. 4, and refs. 19 and 20).

Discussion

In Addition to Its Role as a Liver Tumor Suppressor, TIFα Is Instrumental in Preventing Ectopic Calcifications and Other Features of Premature Aging. The present results show that, in addition to hepatic tumors (6), *TIF1α*$^{-/-}$ mice spontaneously develop pathologic calcifications in arterial vessels, lungs, and vibrissae. Arterial calcifications first appear in the walls of medium-sized arteries and arterioles in the kidney by the age of 3 months and, with aging, they extend to other muscular arteries and become associated with calcifications of lung alveoli and vibrissae capsules. Arterial calcifications vary in prevalence among different organs of *TIF1α*$^{-/-}$ mutants. Liver, spleen, lung, and testis appear relatively resistant to the process, whereas kidney is most vulnerable. Such variation argues against a change in serum pH or ion content as solely responsible for the pathological calcified deposits and favors at least a partial influence from local factors such as vascular dynamics or local differences in endothelial cell metabolic activity.

In mice, arterial calcification is a classical age-related lesion (21), which affects *TIF1α*$^{-/-}$ mutants already 3 months old of age. In this context, it is noteworthy that *TIF1α*$^{-/-}$ mice exhibit other features of premature aging. Among these, lung microlithiasis is present in all *TIF1α*$^{-/-}$ mice as early as 8 months of age while affecting a maximum of 17% WT individuals >25 months

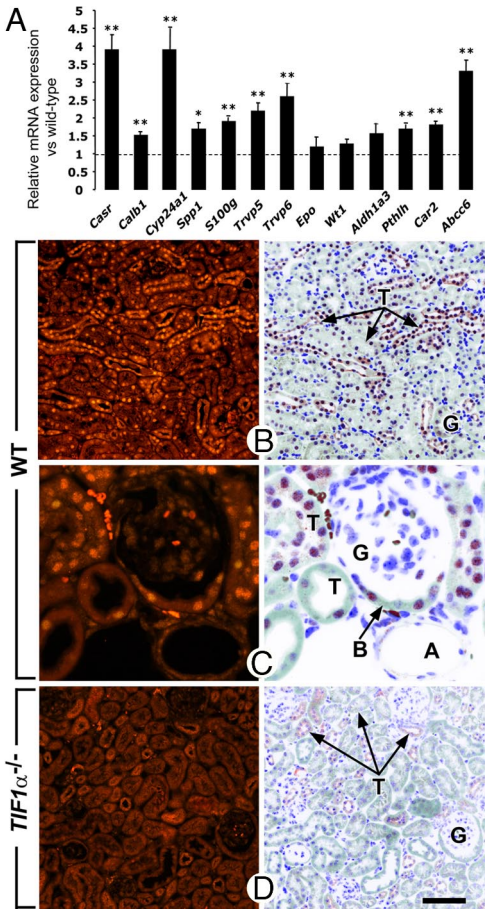

Fig. 3. TIF1α is ubiquitously expressed in nephrons and represses gene expression in kidneys. (*A*) Total RNA extracted from kidneys of 3-month-old WT and *TIF1*$\alpha^{-/-}$ mutants ($n = 4$ in each group) was analyzed by quantitative RT-PCR. Expression of the indicated genes was analyzed in triplicate together with *HPRT*, and results are represented as expression relative to *HPRT* for WT and mutant, with expression of each gene arbitrarily set equal to one for WT samples (indicated by the horizontal dotted line). *, $P < 0.05$; **, $P < 0.01$. (*B–D*) Histological sections through the kidney cortex immunostained with an antibody specific to TIF1α. Genotypes are as indicated. In *D* note the absence of stained nuclei in the TIF1α-deficient kidney. A, arteriole; B, Bowman's capsule of a glomerulus; G, kidney glomeruli; T, kidney tubules. (Scale bar: *B* and *D*, 80 μm; *C*, 20 μm.)

in a strain that is predisposed to this defect (22). Hepatocyte karyo- and cytomegaly, which is present in all *TIF1*$\alpha^{-/-}$ mice as early as 3 months of age (6), is occasionally observed in WT mice >18 months (23). Intranuclear inclusions represent another feature encountered in the liver of aging WT mice that is already present in all *TIF1*$\alpha^{-/-}$ livers at 3 months of age (SI Fig. 5).

The Calcifying Arteriopathy of *TIF1*$\alpha^{-/-}$ Mutant Mice Resembles the Human Mönckeberg's Disease (MD). In humans, diabetes, atherosclerosis, and end-stage renal failure are the most common diseases predisposing arteries to calcification. In *TIF1*$\alpha^{-/-}$ mutants, these diseases can not, however, account for the observed defects. *TIF1*$\alpha^{-/-}$ mutants are not hyperglycemic (Table 1 and ref. 24). Their calcifications never affect large arteries, do not have an inflammatory component, and are not associated with lipid deposits, thus excluding atherosclerosis (25). Moreover, the kidney lesions of *TIF1*$\alpha^{-/-}$ mutants are not extensive enough to yield elevated circulating creatinine concentrations (which attest to renal failure) and do not result in hyperphosphatemia. Thus, the scattered fibrotic glomeruli seen in *TIF1*α-deficient kidneys appears to be a consequence of blocks of renal arterioles by calcified intraluminal deposits and not a cause of renal insufficiency. The normal serum phosphate levels also exclude the involvement of the circulating phosphaturic factor, fibroblast growth factor-23 (FGF-23) (26, 27), in the pathogenesis of the ectopic calcifications of *TIF1*$\alpha^{-/-}$ mutants.

In humans, extensive calcification of the walls of medium sized and small arteries, referred to as MD, is common in the elderly (28). *Per se* MD is most often asymptomatic, but affected arteries may develop atherosclerosis (29). The calcifying arteriopathy of *TIF1*$\alpha^{-/-}$ mutants shares many common features with MD, notably a similar arterial bed, an increase in severity with aging, and a near absence of secondary ischemic lesions. Moreover, MD can occur in individuals without atherosclerostic lesions or metabolic risk factors and with normal blood parameters (30, 31) and can be associated with other sites of ectopic calcifications (31). These characters are also observed in the *TIF1*$\alpha^{-/-}$ arteriopathy, which may thus represent a mouse equivalent of MD.

***TIF1*α May Prevent Soft Tissue Calcifications Through Decreasing *Casr* Expression.** Under certain pathological conditions, some soft tissues and organs, in particular blood vessels, are prone to calcification, and growing evidence suggests that vascular calcification is a highly regulated process, involving both systemic and local inducers and inhibitors (32). Inhibition of soft tissue mineralization is notably achieved through systemically acting serum inhibitors of calcium-phosphate deposition synthesized by the liver such as fetuin-A (α2-HS-glycoprotein) and fetuin-B (11–13). The possibility that a reduced synthesis of mineralization inhibitors of liver origin could account for ectopic calcifications in *TIF1*$\alpha^{-/-}$ mutants appears unlikely, as selective inactivation of *TIF1*α in hepatocytes does not yield these abnormalities.

Osteoprotegerin (Opg; a secreted peptide of the tumor necrosis factor receptor gene superfamily) and matrix Gla protein (Mgp; a structural component of extracellular matrices) appear to inhibit arterial calcifications through their local production by vascular smooth muscle cells, rather than through their remote synthesis and secretion in blood (33–35). As (*i*) the sites and/or nature of arterial defects in *Opg*-null mice (33) and *Mgp*-null mice (34–36) are very distinct from those of *TIF1*$\alpha^{-/-}$ mutants, (*ii*) *Mgp* is normally expressed in the kidneys of 3-month-old *TIF*$\alpha^{-/-}$ mice (unpublished results), and (*iii*) TIF1α is not detected in blood vessel walls, a role for TIF1α in regulating *Opg* and *Mgp* expression appears unlikely. In contrast to *Opg* and *Mpg* knockout mice, ectopic calcifications in *Car2* (37) or *Abcc6* (38–40) knockout mice affect medium-sized arteries and/or vibrissae capsules, thereby showing similarities with those of *TIF1*$\alpha^{-/-}$ mutants. However, expression of *Car2* and *Abcc6*, which is increased in response to *TIF1*α deficiency, is unlikely to be involved in the pathology of *TIF1*$\alpha^{-/-}$ mutants.

The association of ectopic calcifications in arteries, arterioles, vibrissae capsules, and lung alveoli appears to be unique to *TIF1*$\alpha^{-/-}$ mutants (present report) and mouse mutants carrying an activating mutation of the *Casr* gene (41). The latter encodes a G-coupled seven-transmembrane domain protein that plays a central role in controlling calcium homeostasis (42). That *Casr* expression in the kidney is increased upon *TIF1*α ablation raises the possibility that *TIF1*α ablation predisposes to pathological calcification through activation of *Casr* expression.

TIF1α Represses the VDR Signaling Pathway in the Kidney. TIF1α has previously been shown to interact both physically and functionally with the ligand-dependent activation domain AF-2 of numerous nuclear receptors, including VDR (1, 5, 6). Signaling through the VDR plays a critical role in calcium homeostasis (16, 43), and abnormal regulation of vitamin D signaling promotes arterial calcifications (refs. 26 and 44 and references therein).

Table 2. TIF1α is detected in a large variety of epithelia

Epithelia	Signal	Figure
Cardiovascular system		
Myocardium	0	
Arteries and veins (endothelium and smooth muscles)	0	Fig. 3*C*
Capillaries (endothelium)	0	
Respiratory system		
Tracheal epithelium and cartilage	0	
Alveolar epithelium	0	
Digestive system		
Esophagus (epithelium)	+	
Stomach (epithelium of fundic glands)	+	
Ileum (epithelium)	+	
Colon (epithelium)	+	SI Fig. 4*D*
Liver parenchyma	+	
Pancreas (exocrine)	+	SI Fig. 4*E*
Urinary system		
Kidney glumeruli (Bowman's capsules)	+	Fig. 3*C*
Kidney tubules	+	Fig. 3 *B* and *C*
Urinary bladder epithelium	+	
Genital system		
Testis		SI Fig. 4*A*
Sertoli cells	+ +	
Spermatocytes	0 (PR) to + + (D)	
Round spermatids	+ + +	
Leydig cells	0	
Epididymis (epithelium of the head)	+ +	SI Fig. 4*C*
Epididymis (epithelium of the tail)	0	
Vas deferens (epithelium)	+ +	
Cranial prostate (epithelim)	+ +	
Granulosa cells	+	SI Fig. 4*I*
Oocytes	0	
Oviduct (epithelium)	+ +	SI Fig. 4K
Uterus (epithelium and glands)	+ +	SI Fig. 4*J*
Uterus (stroma)	+	SI Fig. 4*J*
Endocrine glands		
Pancreas (Langerhans cells)	+	SI Fig. 4*E*
Parathyroid glands	+	SI Fig. 4*G*
Thyroid gland	0	
Adrenal gland (cortex and medulla)	+	
Miscellaneous connective tissues		
White and brown adipose tissue	0	
Striated muscle (oesophagus)	0	
Skin (epidermis and dermis)	0	

Connective tissues are not stained with the anti-TIF1α antibody with the notable exception of the uterine stroma. Note that tissues of age-matched *TIF1α*$^{-/-}$ mutants were used as negative controls. PR and D, prelepotene and diplotene spermatocytes, respectively. 0, absence of nuclear immunofluorescent signal. +, ++, and +++ indicate increasing intensities of nuclear immunofluorescent signals.

Kidney is a key target organ of the vitamin D endocrine system, and both vitamin D deficiency and VDR ablation lead to impaired renal functions (refs. 43 and 45 and references therein). In this context, it is noteworthy that (*i*) the *Casr* promoter is known to contain functional vitamin D responsive elements, (*ii*) *Casr* mRNA levels in kidney are increased upon vitamin D administration and decreased in *VDR*-null mutant mice (15, 45), and (*iii*) *TIF1α*, *VDR*, and *Casr* all are expressed in distal convoluted tubules (refs. 20 and 46 and Fig. 3 *B* and *C*). We also show that, in addition to *Casr*, expression of other direct vitamin D target genes, including *Car2*, *Cyp24a1*, *Trpv5*, *Trpv6*, *Calb1*, *S100g Spp1*, and *Pthlh*, is up-regulated in kidney upon *TIF1α* ablation. Altogether, these data indicate that TIF1α normally functions to repress the vitamin D endocrine system and additionally suggest that ectopic calcifications in *TIF1α*$^{-/-}$ mice are causally related to a disturbed VDR signaling pathway. Interestingly, the fact that these metabolic disturbances correlate with a calcifying arteriopathy and other features of premature aging in *TIF1α*$^{-/-}$ mice provides support for the hypothesis that aging is promoted by an increased activity of the vitamin D signaling pathway (26, 27).

In conclusion, the present data demonstrate that *TIF1α* plays an indispensable role in regulating a molecular pathway involving VDR and Casr, which functions to prevent ectopic calcifications *in vivo*.

Materials and Methods

Mice. All mice were on a mixed C57BL/6–129/Sv genetic background and housed in an animal facility licensed by the French Ministry of Agriculture (agreement B67-218-5, 1999-02-09). Animal experiments were supervised by M.M. who is qualified for experimenting with mice (French Ministry of Agriculture agreement 67-62, 2003-05-30).

Histology, Alizarin Red-Stained Whole-Mount Preparations, and Immunohistochemistry. Tissues from *TIF1α*$^{-/-}$ mutants and WT littermates were collected at 2, 3, and 8–10 months of age. Tissues were fixed in 4%

(wt/vol) buffered formalin for 24 h, then either embedded in paraffin or frozen in liquid nitrogen vapors (47). Histological sections from paraffin-embedded tissues were stained either with hematoxylin/eosin or processed using the von Kossa method for localizing calcium histochemically (48). In the latter staining method, nuclei were counterstained either with hematoxylin/eosin, safranin O, or DAPI, and the DAPI fluorescence was then converted into a bright-field image with Photoshop (Abode). Organs that were systematically analyzed included: heart, aorta white fat and interscapular brown fat, striated muscle, liver, trachea, lung, kidney, testis, eye and adnexia, thyroid gland tongue spleen, and skin. Oil red O staining of frozen histological sections was performed as described (47). Histological observations were repeated on at least eight males and eight females per genotype and age group. For alizarin red staining of mouse carcasses (comprising bones, striated muscles, and muzzle skin), mice were killed, eviscerated, fixed in ethanol, cleared in KOH, and stained with alizarin red (see *SI Text*). Immunohistochemistry with the monoclonal anti-TIF1α antibody 5T1E8 (1) was performed according to standard protocols (see *SI Text*).

RNA Isolation, Reverse Transcription, and Real-Time PCR Analysis. Total RNA from whole kidneys was isolated by using Rneasy (Qiagen), and 5 μg was used for cDNA synthesis primed with oligo(dT)$_{24}$ (Invitrogen). The final product was then diluted 80 times, and 4 μl was mixed with the forward and reverse primers listed in SI Table 4 (250 nM of each primer at final concentration) and 5 μl of SYBR Green master mix. Real-time PCR was performed with the LightCycler 1.5 system (Roche). Each cDNA sample was tested in triplicate, and the expression level of each gene was normalized to the hypoxanthine-guanine phosphoribosyltransferase level.

Blood Sample Analyses. Blood collection and establishment of biochemical and hematological parameters were as described (49).

ACKNOWLEDGMENTS. We thank M. Cerviño, M. Oulad-Abdelghani, N. Messaddeq, M. F. Champy, and the staff of the Institut de Génétique et de Biologie Moléculaire et Cellulaire and the Institut Clinique de la Souris common services for their technical assistance. This work was supported by the Centre National de la Recherche Scientifique, the Institut National de la Santé et de la Recherche Médicale, the Agence Nationale de la Recherche, the Faculty of Medicine, and the University Hospital of Strasbourg. M.I. was supported by a Charcot fellowship from the French Ministère des Affaires Étrangères. J.T. was supported by the Association pour la Recherche sur le Cancer. K.K. was supported by the Ligue Nationale contre le Cancer and the Armenian Foundation Boghos Noubar Pacha (Belgium).

1. Le Douarin B, *et al.* (1995) TIF1, a potential mediator of the ligand-dependent activation function (AF-2) of nuclear receptors, is fused to B-raf in the oncogenic protein T18. *EMBO J* 14:2020–2033.
2. Le Douarin B, *et al.* (1996) A possible involvement of TIF1α and TIF1β in the epigenetic control of transcription by nuclear receptors. *EMBO J* 15:6701–6715.
3. Zhong S, *et al.* (1999) A RA-dependent, tumor-growth suppressive transcription complex is the target of the PML-RARalpha and T18 oncoproteins. *Nat Genet* 23:287–295.
4. Teyssier C, Ou C-Y, Khetchoumian K, Losson R, Stallcup MR (2006) TIF1α mediates physical interaction and functional synergy between the CARM1 and GRIP1 nuclear receptor coactivators. *Mol Endocrinol* 20:1276–1286.
5. Nielsen AL, *et al.* (1999) Interaction with members of the heterochromatin protein 1 (HP1) family and histone deacetylation are differentially involved in transcriptional silencing by members of the TIF1 family. *EMBO J* 18:6385–6395.
6. Khetchoumian K, *et al.* (2007) Loss of Trim24 (Tif1α) gene function confers oncogenic activity to retinoic acid receptor alpha. *Nat Genet* 39:1500–1506.
7. Starost MF, Benavides F, Conti CJ (2002) A variant of pulmonary alveolar microlithiasis in nackt mice. *Vet Pathol* 39:390–392.
8. Chan ED, Morales DV, Welsh CH, McDermott MT, Schwarz MI (2002) Calcium deposition with or without bone formation in the lung. *Am J Respir Crit Care Med* 165:1654–1669.
9. Moe SM, Chen NX (2004) Pathophysiology of vascular calcification in chronic kidney disease. *Circ Res* 95:560–567.
10. Jono S, Shioi A, Ikari Y, Nishizawa Y (2006) Vascular calcification in chronic kidney disease. *J Bone Miner Metab* 24:176–181.
11. Olivier E, *et al.* (2000) Fetuin-B, a second member of the fetuin family in mammals. *Biochem J* 350:589–597.
12. Denecke B, *et al.* (2003) Tissue distribution and activity testing suggest a similar but not identical function of fetuin-B and fetuin-A. *Biochem J* 376:135–145.
13. Schafer C, *et al.* (2003) The serum protein alpha 2-Heremans-Schmid glycoprotein/fetuin-A is a systemically acting inhibitor of ectopic calcification. *J Clin Invest* 112:357–366.
14. Quélo I, Jurdic P (2000) Differential regulation of the carbonic anhydrase II gene expression by hormonal nuclear receptors in monocytic cells: Identification of the retinoic acid response element. *Biochem Biophys Res Commun* 271:481–491.
15. Canaff L, Hendy GN (2002) Human calcium-sensing receptor gene: Vitamin D response elements in promoters P1 and P2 confer transcriptional responsiveness to 1,25-dihydroxyvitamin D. *J Biol Chem* 277:30337–30350.
16. Christakos S, et *al.* (2006) New insights into the mechanisms involved in the pleiotropic actions of 1,25 dihydroxyvitamin D3. *Ann NY Acad Sci* 1068:194–203.
17. Meyer MB, Zella LA, Nerenz RD, Pike JW (2007) Characterizing early events associated with the activation of target genes by 1,25-dihydroxyvitamin D3 in mouse kidney and intestine *in vivo*. *J Biol Chem* 282:22344–22352.
18. Okazaki T, Nishimori S, Ogata E, Fujita T (2003) Vitamin D-dependent recruitment of DNA-PK to the chromatinized negative vitamin D response element in the PTHrP gene is required for gene repression by vitamin D. *Biochem Biophys Res Commun* 304:632–637.
19. Naveh-Many T, Marx R, Keshet E, Pike JW, Silver J (1990) Regulation of 1,25-dihydroxyvitamin D3 receptor gene expression by 1,25-dihydroxyvitamin D3 in the parathyroid *in vivo*. *J Clin Invest* 86:1968–1975.
20. Suh JM, *et al.* (2006) The expression profiles of nuclear receptors in the developing and adult kidney. *Mol Endocrinol* 20:3412–3420.
21. Pendl J, Kölle S, Sinowatz F, Schmahl W (1996) in *Pathobiology of the Aging Mouse*, eds Mohr D, *et al.* (International Life Sciences Institute, Washington, DC), Vol 1, pp 385–401.
22. Ernst H, Dungworth DL, Kamino K, Rittinghausen S, Mohr U (1996) in *Pathobiology of the Aging Mouse*, eds Mohr D, *et al.* (International Life Sciences Institute, Washington, DC), Vol 1, pp 282–300.
23. Harada T, Maronpot RR, Enomoto A, Tamano S, Ward JM (1996) in *Pathobiology of the Aging Mouse*, eds Mohr D, *et al.* (International Life Sciences Institute, Washington, DC), Vol 2, pp 208–241.
24. Hsueh W, *et al.* (2007) Recipes for creating animal models of diabetic cardiovascular disease. *Circ Res* 100:1415–1427.
25. Abedin M, Tintut Y, Demer LL (2004) Vascular calcification: Mechanisms and clinical ramifications. *Arterioscler Thromb Vasc Biol* 24:1161–1170.
26. Razzaque MS, Sitara D, Taguchi T, St-Arnaud R, Lanske B (2006) Premature aging-like phenotype in fibroblast growth factor 23 null mice is a vitamin D-mediated process. *FASEB J* 20:720–722.
27. Lanske B, Razzaque MS (2007) Vitamin D aging: Old concepts and new insights. *J Nutr Biochem* 18:771–777.
28. Kröger K, *et al.* (2006) Prevalence of peripheral arterial disease: Results of the Heinz Nixdorf recall study. *Eur J Epidemiol* 21:279–285.
29. Kumar V. Robbins SL, Cotran RS (1997) *Basic Pathology* (Saunders, Philadelphia).
30. Lanzer P (1998) Mönckeberg media calcinosis. *Z Kardiol* 87:586–593.
31. Barra Couri CE, *et al.* (2005) Mönckeberg's sclerosis: Is the artery the only target of calcification? *BMC Cardiovasc Disord* 5:34–40.
32. Speer MY, Giachelli CM (2004) Regulation of cardiovascular calcification. *Cardiovasc Pathol* 13:63–70.
33. Bucay N, *et al.* (1998) Osteoprotegerin-deficient mice develop early-onset osteoporosis and arterial calcification. *Genes Dev* 12:1260–1268.
34. Luo G, *et al.* (1997) Spontaneous calcification of arteries and cartilage in mice lacking matrix GLA protein. *Nature* 386:78–81.
35. Murshed M, Schinke T, McKee MD, Karsenty G (2004) Extracellular matrix mineralization is regulated locally; Different roles of two gla-containing proteins. *J Cell Biol* 165:625–630.
36. El-Maadawy S, *et al.* (2003) Cartilage formation and calcification in arteries of mice lacking matrix Gla protein. *Connect Tissue Res* 44:272–278.
37. Spicer SS, Lewis SE, Tashian RE, Schulte BA (1989) Mice carrying a CAR-2 null allele lack carbonic anhydrase II immunohistochemically and show vascular calcification. *Am J Pathol* 134:947–954.
38. Klement JF, *et al.* (2005) Targeted ablation of the ABCC6 gene results in ectopic mineralization of connective tissues. *Mol Cell Biol* 25:8299–8310.
39. Gorgels TG, *et al.* (2005) Disruption of *Abcc6* in the mouse: Novel insight in the pathogenesis of pseudoxanthoma elasticum. *Hum Mol Genet* 14:1763–1773.
40. Jiang Q, Li Q, Uitto J (2007) Aberrant mineralization of connective tissues in a mouse model of pseudoxanthoma elasticum: Systemic and local regulatory factors. *J Invest Dermatol* 127:1392–1402.
41. Hough TA, *et al.* (2004) Activating calcium-sensing receptor mutation in the mouse is associated with cataracts and ectopic calcification. *Proc Natl Acad Sci USA* 101:13566–13571.
42. Brown EM, MacLeod RJ (2001) Extracellular calcium sensing and extracellular calcium signaling. *Physiol Rev* 81:239–297.
43. Demay MB (2006) Mechanism of vitamin D receptor action. *Ann NY Acad Sci* 1068:204–213.
44. Price PA, June HH, Buckley JR, Williamson MK (2001) Osteoprotegerin inhibits artery calcification induced by warfarin and by vitamin D. *Arterioscler Thromb Vasc Biol* 21:1610–1616.
45. Li X, Zheng W, Li YC (2003) Altered gene expression profile in the kidney of vitamin D receptor knockout mice. *J Cell Biochem* 89:709–719.
46. Riccardi D, *et al.* (1998) Localization of the extracellular Ca^{2+}/polyvalent cation-sensing protein in rat kidney. *Am J Physiol* 274:611–622.
47. Mark M, *et al.* (2007) in *Current Protocols in Molecular Biology*, eds Ausubel FM *et al.* (Wiley, New York), pp 1–32.
48. Lillie RD (1965) *Histopathologic Technic and Practical Histochemistry* (McGraw–Hill, New York).
49. Champy MF, *et al.* (2004) Mouse functional genomics requires standardization of mouse handling and housing conditions. *Mamm Genome* 15:768–783.